Journal of Nuclear Materials 449 (2014) 23–30

Contents lists available at ScienceDirect

Journal of Nuclear Materials

journal homepage: www.elsevier.com/locate/jnucmat

Gamma-phase homogenization and texture in U–7.5Nb–2.5Zr (Mulberry) alloy

Denise Adorno Lopes [a,*], Thomaz Augusto Guisard Restivo [a,b], Nelson Batista de Lima [c], Angelo Fernando Padilha [a]

[a] Escola Politécnica USP, Av. Prof. Mello Moraes 2463, 05508-030 São Paulo, SP, Brazil
[b] UNISO, Universidade de Sorocaba, Rod. Raposo Tavares km 92.5, 18023-000 Sorocaba, SP, Brazil
[c] Instituto de Pesquisas Energéticas e Nucleares-IPEN, Travessa R, 400 Cidade universitária, 05508-900 São Paulo, SP, Brazil

ARTICLE INFO

Article history:
Received 29 October 2013
Accepted 17 February 2014
Available online 22 February 2014

ABSTRACT

This work investigates the phenomena of homogenization and texture of the γ phase in U–7.5Nb–2.5Zr (Mulberry) alloy prepared by induction melting and cold-rolling. The microstructural characterization of the as-cast and homogenized alloy (heat treated in γ phase region and then quenched in water), as well as the deformed state, was performed using optical and electron microscopy techniques, hardness testing and X-ray diffraction, employing the Rietveld method. The as-cast microsegregation was qualitatively observed by optical microscopy whereas the quantitative evaluation was obtained by electronprobe micro-analysis (EPMA). The homogenization state of the structure was evaluated after heat treatment at 1000 °C in a tube furnace for 5 h. It was found that this treatment is effective in eliminate dendritic segregation in this alloy.

The texture of the Mulberry alloy was studied by X-ray diffraction (XRD) in the γ-phase stabilized condition and deformed state (rolled at room temperature). The stabilized γ alloy showed moderate texture mainly on the components $(023)\langle 100\rangle$ and $(032)\langle 100\rangle$. After 80% deformation, the sample showed a fiber texture $(001)\langle uvw\rangle$, not commonly found in BCC metals, besides the γ fiber $(111)\langle uvw\rangle$ with intermediate intensity.

1. Introduction

Uranium alloys are considered to be used as fuel for research reactors, to replace the high-enriched reactors (HEU) (>20% U^{235}/U_{tot}) by low-enriched uranium (LEU) (<20% de U^{235}/U_{tot}), a limit that has been established as safe for the non-proliferation of nuclear weapons [1]. Additionally, these fuels are important in the development of new technologies such as fast reactors and compact propulsion reactors [2].

Metallic uranium shows tree polymorphic forms: γ phase (body-center-cubic) above 771 °C, β phase (tetragonal – 30 atoms/cel.) between 665 °C and 771 °C, and α phase (orthorrombic – 4 atoms/cel.) below 665 °C [3]. However, the high temperature γ phase is the only stable one under irradiation while the room temperature α phase structure shows important swelling. Thus, uranium is frequently alloyed with elements such as Nb, Mo, Zr and Ti to stabilize γ phase at lower temperatures. Additionally, this alloying elements are said to improve some properties such as corrosion resistance and mechanical properties [4,5]. In this context, some ternary alloys were developed to contain combined characteristics of the binary systems. The most employed alloy composition is U–7.5Nb–2.5Zr (wt.%) known as Mulberry alloy, which presents a good compromise between mechanical strength, dimensional stability, corrosion resistance, ductility and high density [6–10]. In a previous work [11] the stability of metastable gamma phase of Mulberry alloy was investigated. The results have demonstrated that below 400 °C the alloy does not undergo diffusion-based transformations. This behavior makes Mulberry alloy an alternative as monolithic fuel in research reactors with fuel element plate type, where the temperatures are typically below 200 °C.

Uranium alloys are typically produced by vacuum induction or vacuum arc melting, and cast into molds to produce either engineering components or ingots for subsequent mechanical working [12,13]. Microsegregation of the alloying elements is always present in structures obtained by casting and often remains after cold or hot forming operation inducing constituents in the form of banded regions [14].

Microsegration affects negatively the materials properties such as ductility, tensile strength, corrosion resistance, wear resistance.

* Corresponding author. Tel.: +55 15 981410024.
E-mail address: deniseadorno@hotmail.com (D.A. Lopes).

http://dx.doi.org/10.1016/j.jnucmat.2014.02.030
0022-3115/

It was noted that the elimination of microsegregation can lead to 10% increase in the tensile elongation of U–10%Mo while preserving the ultimate yield strength [15]. Additionally, accurate knowledge of the uranium content of alloys is a requirement for control of fissionable material and the burnup of fuel elements. In this connection the U–7.5Nb–2.5Zr alloys have a large solidification range which may requires special care to obtain a homogeneous material [16].

Heat treatment is often used to reduce the microsegregation in alloys and obtain good properties of the final product or for further mechanical forming. However, this approach may not be feasible due to higher costs related to the temperatures and times required. The procedure of such step for uranium alloys is particularly critical since this metal undergoes severe oxidation, which requires protective atmosphere throughout the entire process [17].

The crystallographic texture is another important factor for processing the fuel element. It is a parameter which can be controlled to confer high resistance to thinning or ensures isotropic properties [18]. It is noteworthy that the texture study can lead to understanding of the practical application of the alloy, as well as to achievement of the mechanisms involved in the polycrystalline change at thermal and mechanical processes during the production of the fuel elements.

Due to the focus on ceramic fuel from the 1960s years there are few recent systematic studies on classical themes like texture in uranium alloys. Additionally, the use of orientation distribution function figures (ODF) – a quantitative approach to texture – first occurred in the early 1970s [19]. As this issue was developed in a period when the uranium alloys research was declining, it has never been addressed for systems of uranium alloys with γ phase stabilized. There are few works in literature dealing with texture, being most part focusing on α and α'' phases [20,21].

In the work reported here, detailed characterization is presented for U–7.5Nb–2.5Zr alloy during crucial stages of manufacturing a monolithic fuel elements plate (fusion, homogenization and mechanical conformation). The objective is to provide a better understanding of the relation between fabrication routes and microstructural evolution.

2. Experimental

The U–7.5Nb–2.5Zr alloy (wt.%) was prepared in a vacuum induction melting furnace. Weighted uranium pieces (99.7% purity) cut from reduced derbies were employed, while the Nb was added as a compacted powder pellet (Aldrich 99.8%) together with Zr sponge (99.6%) reduced from $ZrCl_4$. The uranium metal and alloying elements were cast into graphite crucible under vacuum of 4×10^{-4} bar at a temperature of 1500 °C (measured with optical pyrometer). The cast dwelling time was controlled to minimize carbon contamination, but taken long enough to allow homogenization. The furnace running parameters were set at 35 kW and 3.5 kHz. After holding times at about 10 min, the melt was poured into a rectangular copper mold and cooled to room temperature under vacuum.

Total casting mass was 783.6 g (U = 705.2 g, Nb = 58.8 g and Zr = 19.6 g). The sample plate for rolling process was cut from the induction melted ingot in the longitudinal direction.

The chemical compositions of the cast alloy U–7.5Nb–2.5Zr (nominal composition) was obtained by the quantitative analysis by Inductively Coupled Plasma Optical Emission Spectrometry (ICP-OES). Analyses were performed on two samples, taken from different positions in the longitudinal direction of the casting piece (top and center), to check homogeneity.

After melting, the alloy was heat-treated at 1000 °C for 5 h in argon atmosphere followed by water quenching to obtain a homogeneous microstructure of γ-phase at room temperature.

Table 1
Chemical composition (wt.%) of the induction melted alloy.

U–7.5Nb–2.5Zr top	U	Nb	Zr
	90.03	7.35	2.4
	C	N	O
	0.021	0.0010	0.0042
	Al	Fe	Cu
	85.08 (ppm)	259.01 (ppm)	50.03 (ppm)
U–7.5Nb–2.5Zr center	U	Nb	Zr
	89.83	7.59	2.36
	C	N	O
	0.023	0.0012	0.0040
	Al	Fe	Cu
	97.45 (ppm)	303.16 (ppm)	64.46 (ppm)

The effect of the heat treatment was evaluated by Vickers hardness measurements, loaded with 500 g, as well as the microstructure evolution by optical and electronic scanning microscopy and X-ray diffraction analysis by the Rietveld method using GSAS software [22]. Preparation of samples and microstructure analysis were carried out accordingly to the methodology proposed by Kelly et al. [23].

Cold rolling was performed at a small mill without any lubrication where the pass reductions were set close to 10% giving a total reduction about 80%.

The study of the macrotexture in U–7.5Nb–2.5Zr alloy in γ stabilized and deformed state was performed with an automatic texture goniometer coupled to a Rigaku diffractometer, Model DMAX-2000, installed in X-Ray Diffraction Laboratory of the Center for Science and Technology of Materials at Institute of Nuclear and Energy Research (CCTM-IPEN). The running parameters were Cu Kα radiation, angular step of 5° and counting time of 5 s per step. All measurements were performed on the sample surface plane.

The crystallographic planes chosen to draw the pole figures were (110), (200), (211) and (310), those have been commonly associated to a body-centered cubic structure. The orientation distribution function (ODF) was determined from the generated data at the pole figures, with the computer program PAT [24,25].

3. Results and discussion

3.1. Segregation and homogenization

The chemical analyses (Table 1) demonstrates clearly that even with of the use of a graphite crucible the contamination by carbon is low, suggesting there is little interaction between the liquid metal and the crucible. Additionally, there is no macrosegregation in

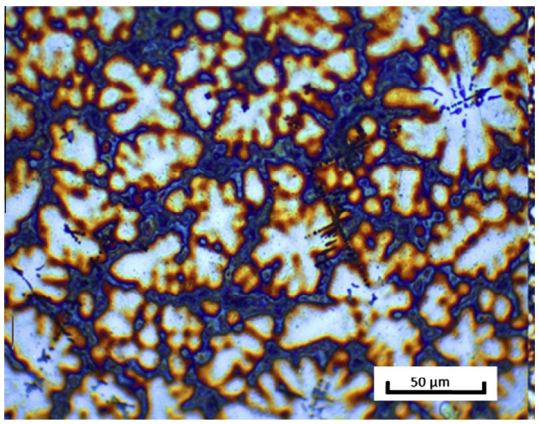

Fig. 1. Optical micrography of the as-cast alloy (500×).

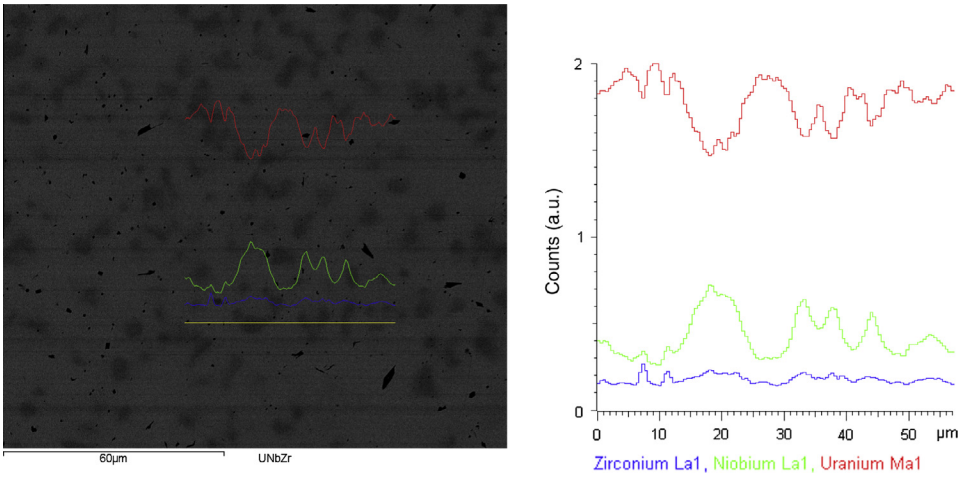

Fig. 2. U–7.5Nb–2.5Zr microprobe analysis at SEM–EDS.

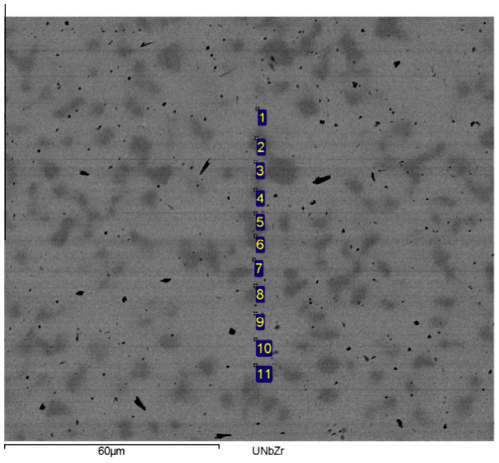

Spectrum	Zr (wt%)	Nb (wt%)	U (wt%)
1	1.35	4.54	94.11
2	3.39	17.97	78.64
3	1.40	7.15	91.45
4	3.40	18.26	78.34
5	2.18	10.43	87.38
6	3.15	16.42	80.43
7	1.78	6.92	91.30
8	5.84	11.25	82.92
9	1.10	6.08	92.83
10	1.35	3.68	94.97
11	1.37	6.43	92.20

Fig. 3. Quantitative evaluation of segregation fields (weight%).

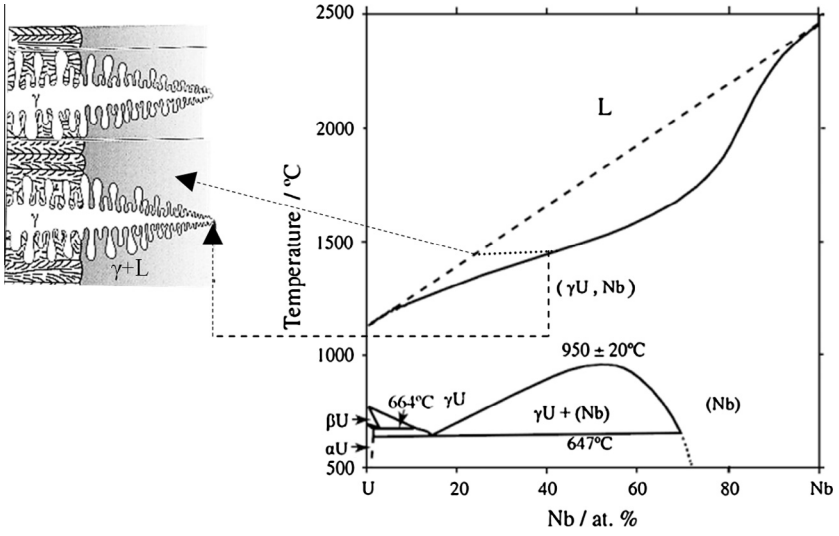

Fig. 4. Schematic illustration of the solidification mode for U–Nb alloys, with dendrites enriched in alloying element.

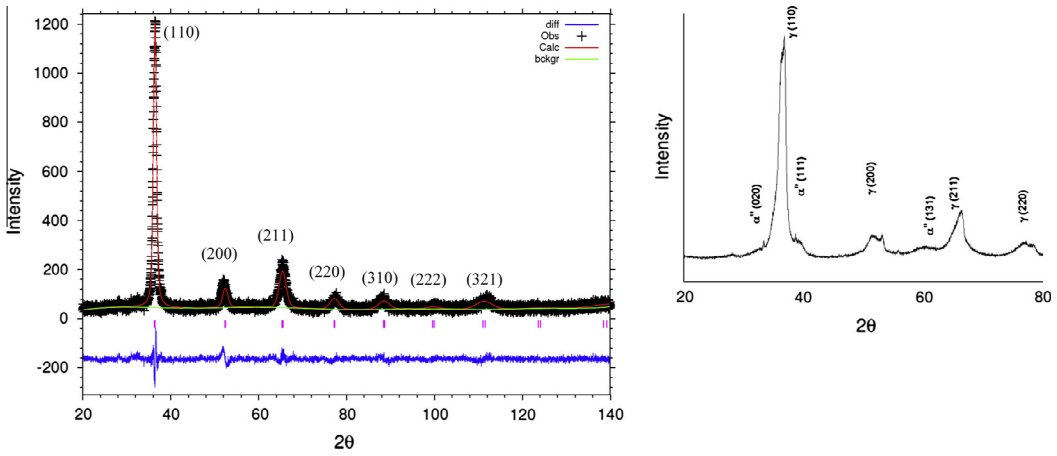

Fig. 5. Rietveld refinement analysis of X-ray for the alloy U–7.5Nb–2.5Zr under γ-phase stabilized state (left) and as-cast state (right).

Table 2
Average Vickers hardness of the alloy in the as-cast and γ-phase quenched condition.

Alloy	Vicker hardness (kg/mm^2)	
U–7.5Nb–2.5Zr	Present work	Vandermeer [10]
As-cast	250.13 (±29.15)	
γ-phase quenched	173.93 (±4.82)	181

the ingot obtained, since the compositions were very close to the nominal one in both regions analyzed.

Fig. 1 presents a view of the obtained alloy in the as-cast condition, using optical microscopy and metallographic etching.

It can be observed that the sample has a microstructure consisting of cellular dendrites which are an indication of intragrain dendritic segregation in the alloy. The metallographic etching produces contrast in microsegration samples because different concentrations of alloying elements leads to different corrosion behaviors. In Fig. 1 the difference of colour tone in dendritic and interdendritic regions is clearly visible, highlighting the occurrence of microsegregation.

One more quantitative view of the microsegregation phenomenon is obtained by chemical microanalysis in the scanning electron microscope. Through this analysis it was observed that the dendritic regions are enriched regarding the alloying elements Nb and Zr. The profile concentration of the elements U, Nb and Zr along a scan line is presented in Fig. 2.

The experimental results obtained along a scanning line related to the maximum and minimum elements concentration (wt%) U, Nb and Zr were 94.97 and 78.34 for uranium, 18.26 and 3.68 for niobium, and 5.84–1.10 for zirconium, as shown in Fig. 3. This result further demonstrates the significant occurrence of microsegregation.

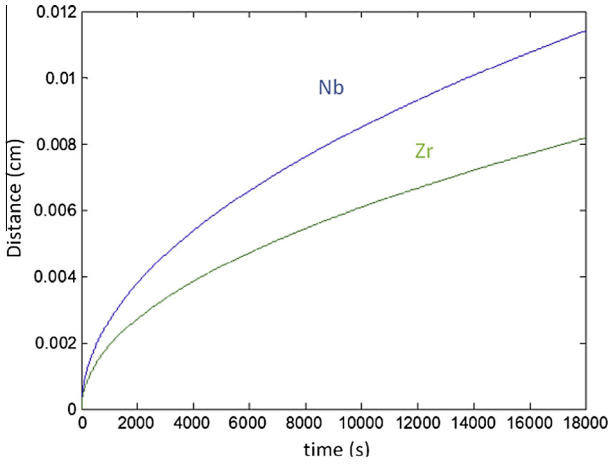

Fig. 7. Diffusion distance for Nb and Zr alloying elements in U γ-phase at 1000 °C.

Based on the binary phase diagram as shown in Fig. 4 [26], specifically the area of separation between liquid and solid, we can make an analysis of the microsegregation results. The phase diagram U–Nb (Fig. 4) shows that a solid and a liquid in equilibrium at certain temperature have different composition. As a consequence the central region of the dendrite, that is the first part to solidify, containing a higher content of niobium than the boundary region in agreement

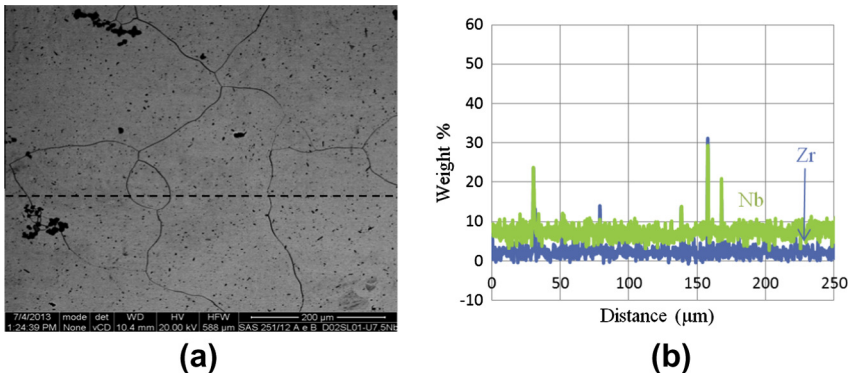

Fig. 6. Back-scattered SEM micrography (dashed line indicate de line scan, direction scan left to right) (a) and chemical microanalysis (b) for heat-treated homogenized U–7.5Nb–2.5Zr alloy.

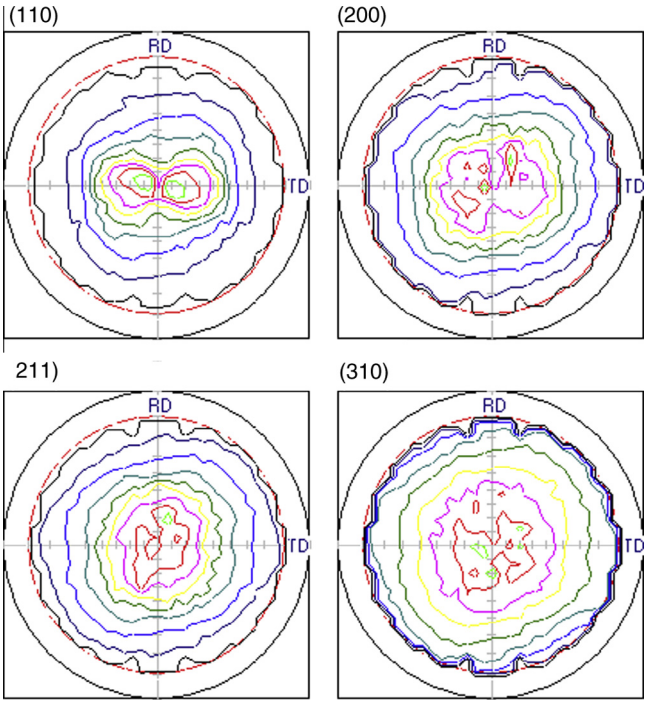

Fig. 8. Pole figures (110), (200), (211) and (310) for γ-stabilized alloy.

with the experimentally observed. Thus, the solution formed in the process of solidification is supersaturated, as a consequence of the relatively low diffusion rates within the solid.

The γ phase stabilization after homogenization heat treatment follow by water quenching can be detected with the aid of the X-ray diffraction. The resulting diffraction pattern is shown in Fig. 5, in comparison with the as-cast diffraction.

The measured diffraction angles correspond to a body-centered cubic structure where the lattice parameter was estimated at about 3.50 Å, by the Rietveld method. It is possible to note a strong broadening of diffraction peaks which can be associated with a high residual stress microstructure that is usual for materials whose have undergone martensitic transformation. Furthermore, it was observed by Rietveld refinement that the peak related to experimental plane (200) is slightly shifted with respect to the standard calculated for an ideal BCC structure (Fig. 5 left). The results indicate the retention of a modified structure similar to the γ equilibrium phase, possibly γ^s, similar to the one related in literature [27].

Vickers hardness test showed the efficiency of heat treatment on alloy homogeneity, reducing the measurements deviation with respect to that observed in the as-cast condition. The lowest hardness value obtained to the stabilized γ-phase reflects the superior plastic behavior of this structure; this was expected since this phase has a structure with many slip systems. Table 2 shows the Vickers hardness values obtained for the alloy in the as-cast and homogenization states in a comparative way with a reference value.

The elimination of the dendritic structure is also evident in the analysis by scanning electron microscopy with backscattered electrons, where it is not observed any contrast difference in the matrix (Fig. 6a). The chemical microanalysis (Fig. 6b) showed significant reduction in microsegregation observed prior to heat treatment. The average mass compositions obtained along the scan line were 7.58% and 2.51% (wt%) for niobium and zirconium respectively. Significant variations in composition can be observed only in points where precipitates rich in Nb an Zr are located.

Homogenization heat treatment typically consist of heating the material to a temperature close to solidus curve, where it rests for a period and follow by a cooling at a predetermined rate. In general, the coarser the dendritic structure the larger the segregation, the more difficult is to homogenize since the distance which must be overcome by diffusion of atoms becomes larger. At high tempera-

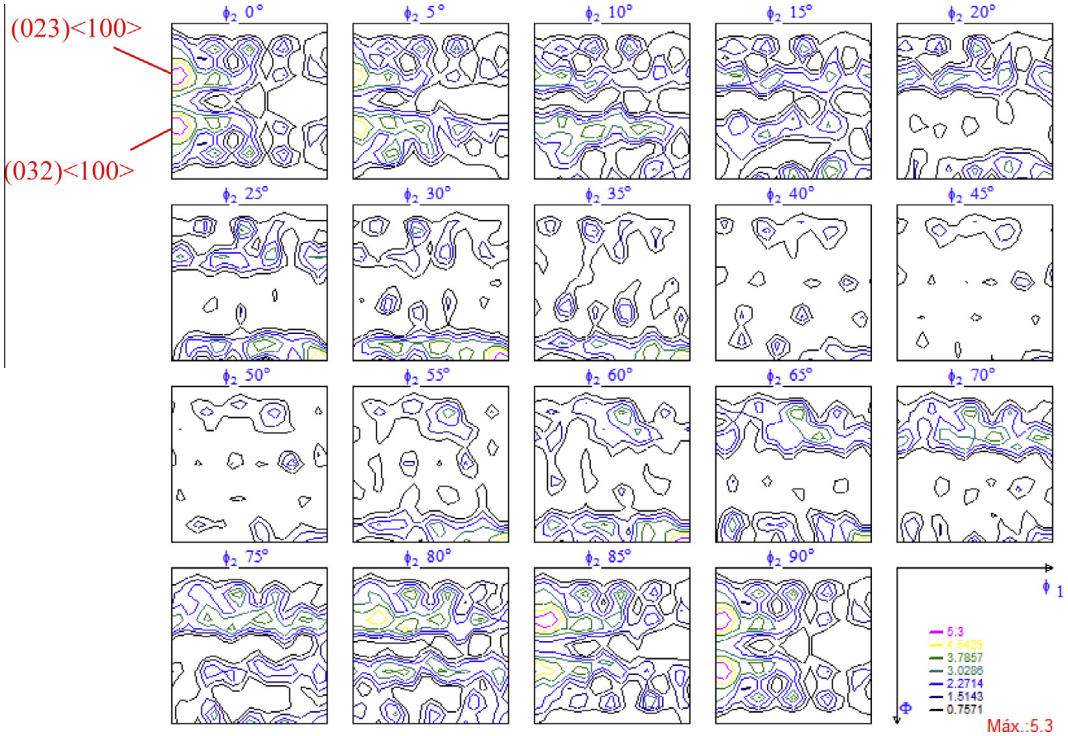

Fig. 9. ODF graphic for the γ-stabilized alloy.

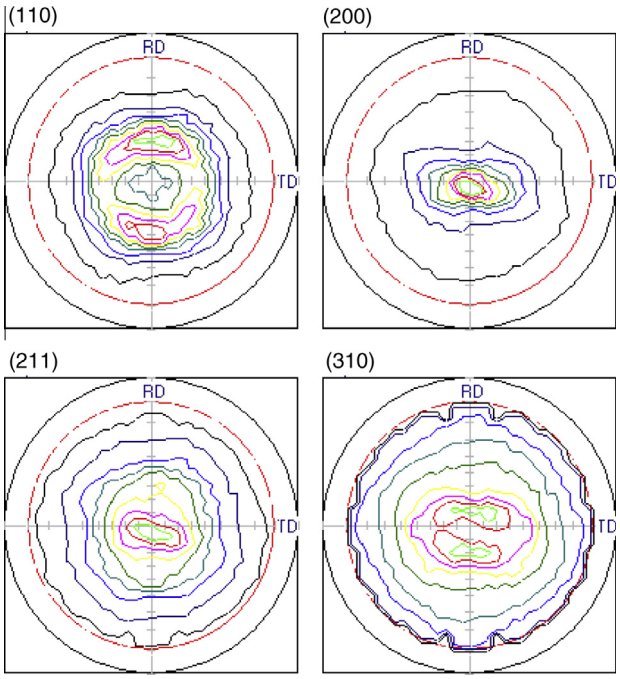

Fig. 10. Pole figures (110), (200), (211) and (310) for the deformed γ -stabilized and cold rolled alloy (80% reduced).

ture the diffusion is enhanced and all the gradient concentration in the alloy decreases. Thus, considering the diffusion coefficient of niobium [28] and zirconium [29] in γ uranium given by the following equations:

$$D_{\gamma}^{Nb} = 4.87 \times 10^{-2} \exp(-39650/RT) \quad (1)$$

$$D_{\gamma}^{Zr} = 0.46 \exp(-47000/RT) \quad (2)$$

One obtains the following diffusion coefficients $D_{\gamma}^{Nb} = 7.25 \times 10^{-9}$ cm/s² and $D_{\gamma}^{Zr} = 3.71 \times 10^{-9}$ cm/s² at 1000 °C. The 2nd Fick law equation can be applied:

$$X^2/t = D_o e^{(-Q/RT)} \quad (3)$$

Considering the 5-h time for heat-treating at 1000 °C, Eq. (3) calculates diffusion distances of approximately 114 and 80 μm for niobium and zirconium, respectively, as plotted in Fig. 7. Both values are higher than the average dendritic size (~50 μm), showing agreement with the experimental results.

Based on the experimental results, the work showed that the microsegregation in U–7.5Nb–2.5Zr alloys can be removed by heat treatment at usual temperatures of industrial furnaces.

3.2. Texture

Figs. 8–11 show the pole figures and ODF obtained for γ-phase stabilized U–7.5Nb–2.5Zr alloy and after cold-rolling at room temperature with a reduction of 80% in thickness approximately.

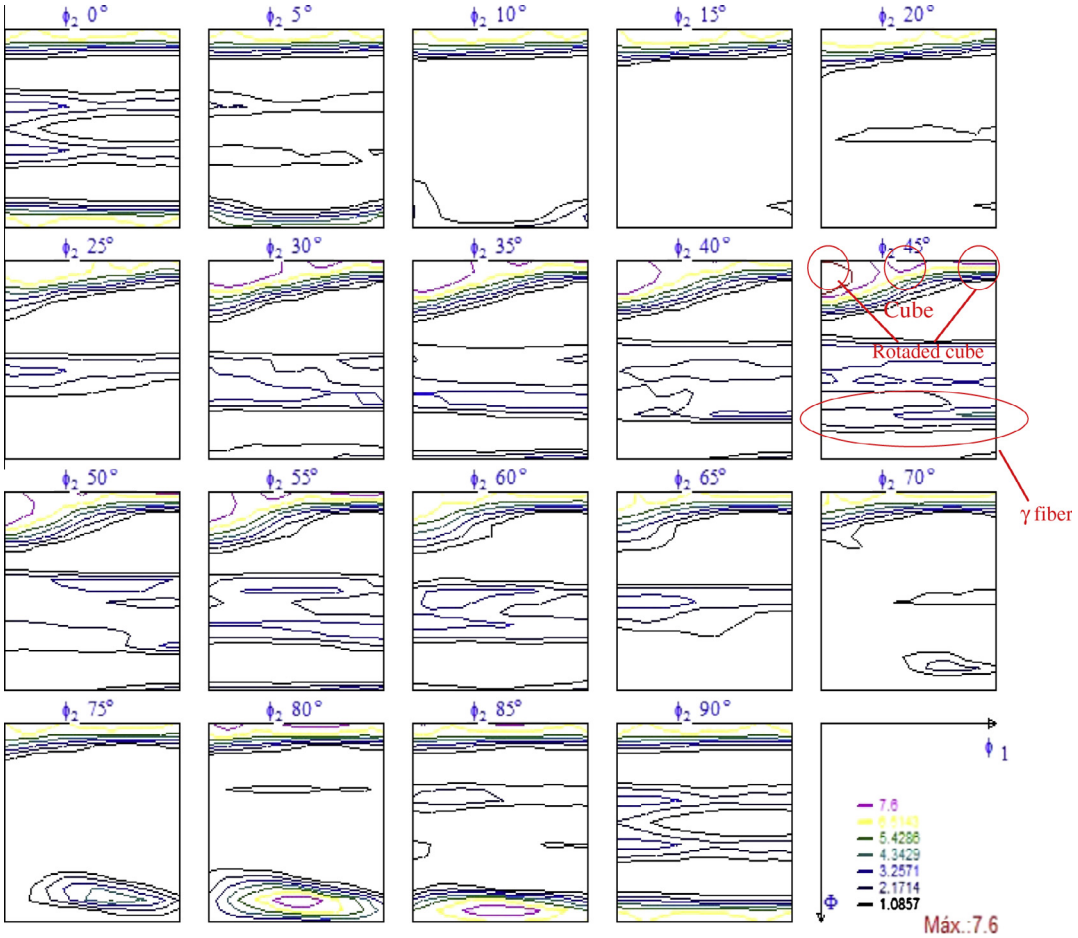

Fig. 11. ODF for the deformed alloy 80% reduction in area.

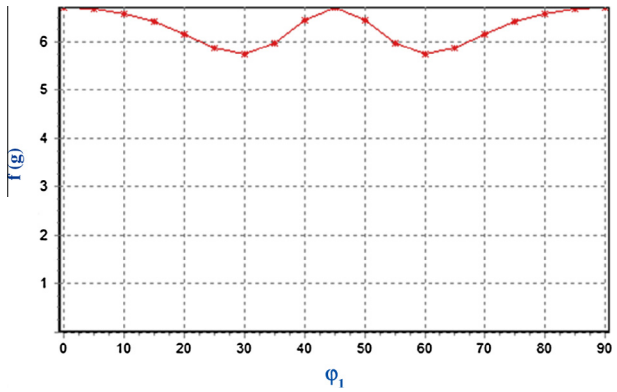

Fig. 12. Fiber (001) ($\Phi = 0°$, $\varphi_2 = 45°$) for the alloy U–7.5Nb–2.5Zr with retained γ-phase, cold rolled up to 80% reduction.

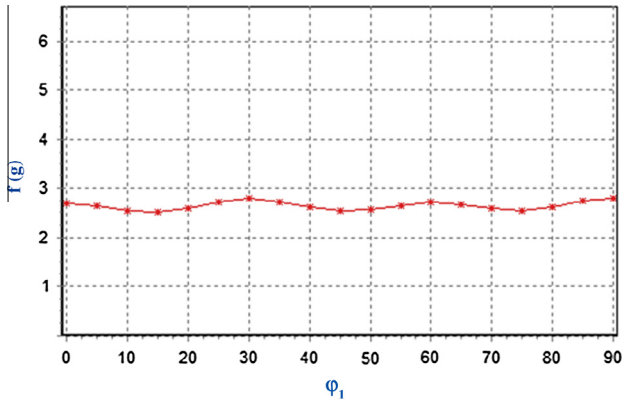

Fig. 13. γ fiber (111)⟨u vw⟩($\Phi = 55°$, $\varphi_2 = 45°$) for the alloy U–7.5Nb–2.5Zr with retained γ-phase cold-rolled up to 80% reduction.

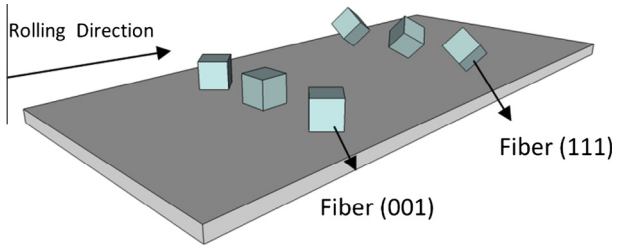

Fig. 14. Schematic representation of the texture components in the rolled plate.

The orientation distribution function (Fig. 9) calculated from the pole figures shows that the alloy in the γ stabilized state at room temperature (obtained by melting, casting, homogenization and then quenching) has texture component composed of (023)⟨100⟩ and (032)⟨100⟩.

After cold-rolling, the U–7.5Nb–2.5Zr alloy showed the emergence of rotated cube textures components {001}⟨1 −10⟩(6.70 times random) and {001}⟨0 −10⟩(6.70 times random). This reveals that the plane (001) was parallel to the rolling direction and rotated in different directions, characterizing a fiber (001)⟨u v w⟩, unusual in BCC materials [30]. This texture possibly shows isotropic properties on the entire plate.

It was also observed that the deformed alloy shows a horizontal band in $\varphi_2 = 45°$ and $\Phi \sim 55°$, with intermediate intensity (2.8 times random), which extends through all values of φ_1. Such occurrence is known as γ fiber and is described as a fiber texture with complete ⟨111⟩ parallel to the normal direction of the plate.

Figs. 12 and 13 evidence the fibers (001)⟨u vw⟩ and γ (111)⟨u vw⟩ in the deformed alloy. The fiber (001) has maximum components in the ⟨110⟩ and ⟨100⟩, and γ fiber shows no strong components along φ_1.

The cold rolling textures of the body-centered cubic materials are characterized by their broad lines located in two partial fibers: {hkl}⟨110⟩, named α fiber, and {111}⟨u vw⟩ γ fiber. The occurrence of the fiber (001)⟨u vw⟩ in the alloy may be associated with factors such as stacking fault energy, indicating the operating slip systems are different from those commonly reported for BCC materials such as ferritic steel for example.

It is noteworthy that the texture measures were performed on the sample surface and, additionally to the low penetration of X-rays in uranium, the texture measured reflect the action of shear stresses.

From the obtained data it is possible to display the following summary of rolled plate (Fig. 14).

Through the Fig. 14 it can be seen that both texture components developed in the rolling process provide isotropic properties along the rolling and transverse directions. This property is of significant technological interest because can provide isotropic behavior in swelling irradiation and thermal expansion, very important factors inside the reactor, where the fuel element must maintain its mechanical stability and, at the same time, incorporate the fission products in its matrix. The uniform distribution of fission gas is desirable for monolithic fuel configuration because in this configuration the fission gas not have the tendency to coalesce into large pockets that are indicators of swelling [31].

Through these data it can be assumed, for example, a manufacturing route that preserves the deformed texture of the fuel using a final heat treatment of relief stress and not recrystallization at higher temperatures.

These data present an unprecedented contribution to the literature since ODF has never been addressed for system of uranium alloys with γ stabilized phase.

4. Conclusions

The experiences and discussions in this paper allow the following conclusions:

(a) The microstructure of the U–7.5Nb–2.5Zr alloy obtained by induction melting method is composed of dendrites, supersatured in the alloys elements, in the as-cast state being necessary to implement homogenization heat treatment.
(b) Heat treatment at 1000 °C for 5 h followed by quenching in water was effective to homogenize the alloy (elimination the dendritic structure) and to retain the cubic structure at room temperature.
(c) Induction melting followed by casting and homogenization heat treatment with quenching in water, produced a moderate texture with the components (023)⟨100⟩ and (032)⟨100⟩.
(d) The cold rolled U–7.5Nb–2.5Zr alloy leads to the emergence of a fiber (001)⟨u vw⟩, with higher intensity, unusual in BCC metals and γ (111)⟨u vw⟩ with moderate intensity. These textures confer isotropic mechanical properties which is very important for a nuclear fuel.

References

[1] Research reactor core conversion from the use of highly enriched uranium to the use of low enriched uranium fuels, guidebook addendum, Heavy water

moderator reactors, IAEA-TECDOC-324, Reduced Enrichment for Research and Test Reactors (RERTR), May 2009 <http://www.rertr.anl.gov>.
[2] G.L. Hofman, L.C. Walters, in: B.R.T. Frost (Ed.), Materials science and Technology: Comprehensive Treatment, Nuclear Materials Part 1, vol. 10A, Wiley VCH, Germany, 1994.
[3] A.N. Holden, Physical Metallurgy of Uranium, Springer, 1958. pp. 1–6.
[4] J.J. Berke, Microstruc. Sci. 7 (1979) 133.
[5] K.H. Eckelmeyer, Uranium and Uranium Alloys, in: ASM Handbook volume 2, Properties and Selection: Nonferrous Alloys and Special Purpose Materials, American Society of Metals, Metals Park, Ohio, 1990.
[6] C.A.W. Peterson, R.R. Vandervoot, The Properties of a Metastable Gamma-phase Uranium Based Alloy: U–7.5Nb–2.5Zr, Lawrence Radiation Laboratory, UCRL-7869, University of California, Livemore, 1964.
[7] C.W. Dean, A Study of the Time-Temperature-Transformation Behavior of a Uranium–7.5 Weight Percent–2.5 Weight Percent Zirconium Alloy, Y – 1 6 9 4, Union Carbide Corporation-Nuclear Division, Oak Ridge Y-12 Plant, Tennessee, 1969. October 24.
[8] F. Giraud-Heraud, J. Guillaumi, Act. Metall. 21 (1973) 1243.
[9] M.M. Karnowsky, R.W. Rohde, J. Nucl. Mater. 49 (1973) 81.
[10] R.A. Vandermeer. Recent observation of phase transformation in a U–Nb–Zr Alloy, in: Proc. Conference on the Physical Metallurgy of Uranium Alloys, Vail, Colorado, Feb. 11–14, 1974.
[11] D.A. Lopes, T.A.G. Restivo, A.F. Padilha, J. Nucl. Mater. 440 (2013) 304–309.
[12] W.D. Wilkinson, Uranium Metallurgy, first ed., vol. 1, Interscience Publishers, New York, 1962.
[13] Metallurgical Technology of Uranium and Uranium Alloys, vols. 1–3, American Society for Metals, 1982.
[14] M.C. Flemings, Mod. Castings 46 (1) (1964) 353–362.
[15] C.P. Coughlen, P.A. Evans, A.B. Townsed, Homogenization evaluation of a cast uranium molybdenum alloy, Y-12 (TID-4500), 1969.
[16] A. Couterne, C. Collot, C. Guillaume, J. Nucl. Mater. 56 (1975) 169–194.
[17] L.J. Weirick, Corrosion of Uranium and Uranium Alloys, In: Corrosion vol. 13, Metals Handbook, ninth ed, American Society for Metals, 1987, p. 813. p. 813.
[18] H.J. Bunge, Texture Analysis in Materials Science, Butterworths, 1982.
[19] H.J. Bunge, Mathematische Methoden der Textureanalyse, Akademie Verlag, 1969.
[20] R.D. Field, D.W. Brown, D.J. Thoma, Philos. Mag. 85 (2005) 2593–2609.
[21] D.W. Brown, M.A.M. Bourke, R.D. Field, W.L. Hults, Mat. Sci. Eng. A 421 (2006) 15–21.
[22] A.C. Larson, R.B. Von Dreele, General Structure Analysis System (GSAS), Los Alamos National Laboratory Report LAUR 86-748, Los Alamos, USA, 2004.
[23] A.M. Kelly, R.D. Field, D.J. Thoma, J. Nucl. Mater. 429 (2012) 118–127.
[24] N. B Lima, Influência da textura em medidas de tensão residual. Instituto de Pesquisas Energéticas e Nucleares (IPEN), PhD Thesis, São Paulo, 1991.
[25] E. Galego, Desenvolvimento de programa computacional para tratamento de dados de textura obtidos pela tecnica de difração de raios X, Instituto de Pesquisas Energéticas e Nucleares (IPEN), M. Sc. Thesis, São Paulo, 2004.
[26] X.J Liu, Z.S. Li, J. Wang, C.P. Wang, J. Nucl. Mater. 380 (2008) 99–104.
[27] H.L. Yakel, J. Nucl. Mater. 33 (1969) 286–295.
[28] N.L. Peterson, S.J. Rothman, Phys. Rev. 136 (1964) A842–A849.
[29] S.J. Rothman, Diffusion in Uranium, its Alloys, and Compounds, Argonne National Laboratory, Illinois, 1961 (ANL-5700 (Pt.C)).
[30] D. Raabe, K. Lücke, Mat. Sci. Technol. 9 (1993) 302–312.
[31] G.L. Hofman, J. Nucl. Mater. 140 (1986) 256.